

Quasi-Zenith Satellite System-based Tour Guide Robot at a Theme Park

Kohei Matsumoto¹, Hiroyuki Yamada¹, Masato Imai¹, Akihiro Kawamura²,
Yasuhiro Kawauchi³, Tamaki Nakamura³, and Ryo Kurazume²

Abstract—For autonomous service robots used in our daily environment, such as a personal mobility vehicles or delivery robots, localization is one of the most important and fundamental functions. A number of localization techniques, including simultaneous localization and mapping, have been proposed. Although a Global Navigation Satellite System (GNSS) is most commonly used in outdoor environments, its accuracy is around 10 meters and so is inadequate for navigation of an autonomous service robot. Therefore, a GNSS is usually used together with other localization techniques, such as map matching or camera-based localization. In the present study, we adopt the Quasi-Zenith Satellite System (QZSS), which became available in and around Japan on November 2018, for the localization of an autonomous service robot. The QZSS provides high-accuracy position information using electronic reference points and four quasi-z Zenith satellites, and has a localization error of less than 10 centimeters. In the present paper, we compare the positioning performance of the QZSS and real-time kinematic GPS, and verify the stability and the accuracy of the QZSS in an outdoor environment. In addition, we introduce a tour guide robot system using the QZSS and present the results of a guided tour experiment in a theme park.

I. INTRODUCTION

Localization is one of the most important and fundamental functions for an autonomous service robot. In an outdoor environment, a Global Navigation Satellite System (GNSS), in particular, the Global Positioning System (GPS), is the most popular technique. However, the accuracy of a GNSS is approximately 10 meters, which is inadequate for navigation of an autonomous service robot. Therefore, real-time kinematic GPS (RTK-GPS) or a virtual reference station (VRS) that provides centimeter-class positioning is used for accurate navigation of an autonomous service robot, such as a personal mobility vehicle or a delivery robot. A number of autonomous robot systems using RTK-GPS have been proposed[1][2][3][4][5]. In [1], the authors proposed the robust and precise localization system that achieves centimeter-level accuracy in diverse city scenes. In this system, the measurement of RTK-GNSS, LiDAR, and IMU are synthesized in the sensor fusion framework using the error-state Kalman filter. In [2], the authors proposed the high-precision localization method by treating the global pose

¹Kohei Matsumoto, Hiroyuki Yamada, Masato Imai are with Graduate School of Information Science and Electrical Engineering, Kyushu University, Fukuoka 819-0395, Japan {matsumoto, yamada, imai}@irvs.ait.kyushu-u.ac.jp

²Akihiro Kawamura and Ryo Kurazume are with Faculty of Information Science and Electrical Engineering, Kyushu University, Fukuoka 819-0395, Japan {kawamura, kurazume}@ait.kyushu-u.ac.jp

³ Yasuhiro Kawauchi and Tamaki Nakamura are with Living Robot Inc., 1-10-8, Plug and Play Shibuya, Dogenzaka, Shibuya, Tokyo 150-0043, Japan {kawauchi.yasuhiro, nakamura.tamaki}@livingrobot.co.jp

estimation problem as a pose graph optimization problem. RTK-GPS and wheel odometry are utilized as constraints of the pose graph. In [3], the authors proposed a sensor fusion method for 3D mapping and localization using multiple heterogeneous and asynchronous sensors. In this system, firstly, they create an accurate prior map by ORB-SLAM [6] and LOAM [7] using a vehicle that has a RTK-GPS sensor unit. After creating the prior map, they use it to localize in the GPS frame of reference without the use of GPS, and thus the localization in GPS-denied environments such as tunnels or parking garages is also performed. In [4], an integrated framework for underground 3D mapping using a mobile rover is proposed. This framework conducts 3D underground mapping based on GPR (Ground Penetrating Radar) data. In this system, RTK-GPS is used for accurate geo-reference. In [5], the underwater localization system for underwater Mining Vehicle (MV) and surface Launch and Recovery Vessel (LARV) is proposed. LARV is used for supporting MV. In this system RTK-GNSS is used for the localization of LARV using RTKLIB [8].

RTK-GPS uses two modules called base and rover stations. The measurement by the base station, which is located in a known position, is used to remove the measurement error due to the influence of the ionosphere and to correct the measurement by the rover station. Since the error compensation technique uses two modules, RTK-GPS can provide centimeter-class accuracy for positioning in an outdoor environment. However, we have to prepare two GNSS modules in this system, and the distance between the base and rover stations is limited to within the communication range between the two modules.

On the other hand, the Quasi-Zenith Satellite System (QZSS) [9] began operating on November 2018 in and around Japan. The QZSS provides high-accuracy position information and a localization error of less than 10 centimeters by using electronic reference points and using four quasi-z Zenith satellites. These satellites transmit signals not only for localization but also for error correction using the electronic reference points. Therefore, we do not need the base station required by RTK-GPS, and thus centimeter-class positioning by QZSS is available using a single module. Since QZSS can be used without the communication between the two stations required for RTK-GPS, QZSS is suitable for mobile robots that move over a wide area, such as the tour guide robot system proposed in this paper.

In the present paper, we compare the positioning performance of RTK-GPS and QZSS, and verify the stability and accuracy of QZSS in an outdoor environment. In addition,

we introduce a tour guide robot system using QZSS and present a guided tour experiment in a theme park.

II. CENTIMETER-CLASS POSITIONING BY GNSS

For high-accuracy measurement using GNSS, error correction is very important. Errors include the clock error of the satellite, the clock error of the receiver, the position error of the satellite, ionospheric delay, tropospheric delay, the effect of multiple paths, and the noise of the receiver [10][11]. In this section, we explain the measurement procedure and the error correction system for RTK-GPS and QZSS.

A. Real-time kinematic GPS

Real-time kinematic GPS (RTK-GPS) uses two modules: a base station and a rover station. Using these modules, RTK-GPS calculates the double difference of the carrier phase and achieves high-accuracy measurement. The double difference of the carrier phase is calculated using the carrier phase from two satellites to base and rover stations. Here, the carrier phase data arriving at the base station from satellite A and satellite B are denoted as (ϕ_r^A and ϕ_r^B), respectively. The double difference of the carrier phase $D\phi_{br}^{AB}$ is calculated as $D\phi_{br}^{AB} = (\phi_r^A - \phi_b^A) - (\phi_r^B - \phi_b^B)$. This calculation removes the clock errors of the satellites and the receiver. In addition, if the distance between the base and rover stations is less than a certain value, the ionospheric delay and tropospheric delay can be removed. Furthermore, by using information on pseudo-ranges between multiple satellites and receivers, we can determine the integer ambiguities remaining as errors and thereby realize centimeter-class positioning. In the present paper, we use MJ-2001-GL1 (Magellan Systems Japan Inc., Fig. 1) as an RTK-GPS module in the experiment.

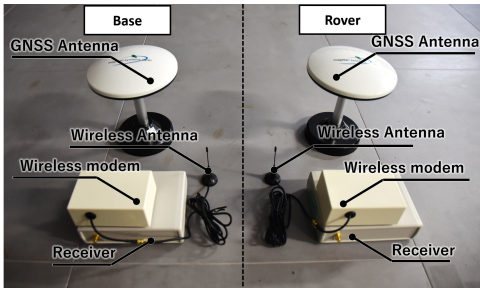


Fig. 1. Real-time kinematic GPS module (MJ-2001-GL1, Magellan Systems Japan Inc.)

B. Quasi-Zenith Satellite System

The QZSS uses four quasi-z zenith orbit satellites, referred to as the "Michibiki" constellation, and began operating in November 2018 in Japan. Whereas RTK-GPS uses two sets of modules, QZSS provides highly accurate positioning with only one module, consisting of an antenna and a receiver. As explained above, the RTK-GPS uses the correction signal measured by the base station. On the other hand, QZSS generates an error correction signal using observation data at electronic reference points placed very densely in Japan, and the correction is performed by transmission to the user terminal via the satellites. This correction method is

referred to as centimeter level augmentation [12] [13], and the centimeter-class positioning has been realized in and around Japan. The quasi-z zenith orbit is shown in Fig. 2. This orbit is an asymmetrical trajectory, and each QZS follows this trajectory in one day. By constructing this quasi-z zenith orbit with four satellites and shifting their positions in time, a high elevation angle to at least one QZS can always be obtained in and around Japan.

In the present paper, we use the QZSS module called AQLOC-V (Mitsubishi Electric Inc., Fig. 3).

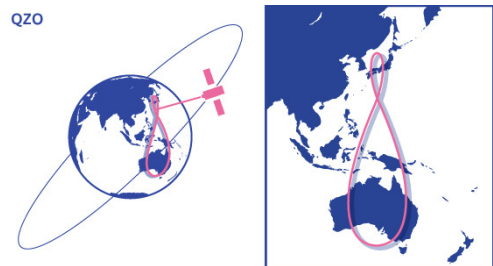


Fig. 2. Quasi-z zenith orbit [14]



Fig. 3. Quasi-Zenith Satellite System module (AQLOC-V, Mitsubishi Electric Inc.)

1) *Centimeter-level augmentation service*: The centimeter level augmentation service (CLAS) is a unique function of QZSS. The "Michibiki" constellation adopts a state space representation (SSR) method [15] for CLAS and realizes centimeter-class positioning using the L6 signal, which is an auxiliary signal of a QZS. In the centimeter-class augmentation information generated at the control segment, a dynamic error model called the state space model (SSM) is used based on observation data of the electronic reference point network. Each error amount, such as the clock error, the satellite orbit error, ionospheric delay, tropospheric delay, and signal bias, is generated as an SSR. The flow of centimeter level augmentation is shown in Fig. 4.

Based on the positioning information at the electronic reference point for which the latitude and longitude are known, the correction information for removing the error is created at a facility called the monitoring station and transmits the information to the quasi-z zenith satellite via the antenna of the tracking station. Then, by receiving the correction information simultaneously with the positioning signal on the user terminal side, centimeter-class positioning is realized.

III. ACCURACY MEASUREMENT EXPERIMENTS

In order to verify the measurement accuracy of QZSS, we compared the positioning performance RTK-GPS and

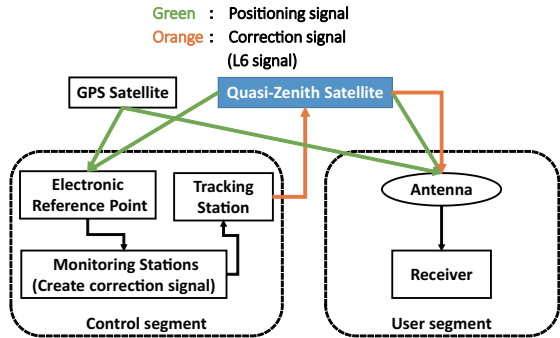


Fig. 4. Flow of centimeter-level augmentation

QZSS in the stand-still state and in motion in an open-sky environment and a partially obscured environment in which buildings block portions of the sky.

A. Measurement accuracy in the stand-still state in an open-sky environment

In this experiment, the distributions of positioning data from the average value by RTK-GPS and QZSS were compared in the stand-still state. The results are shown in Figs. 5 and 6, respectively.

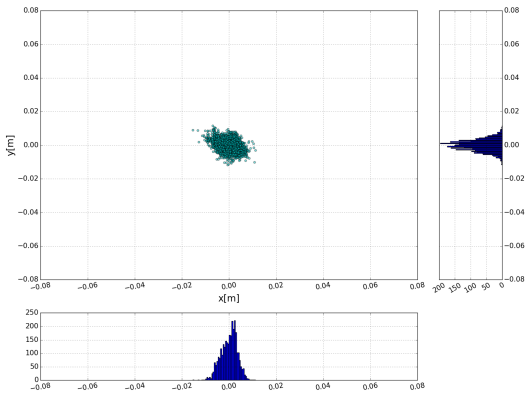


Fig. 5. Distribution of positioning data by RTK-GPS

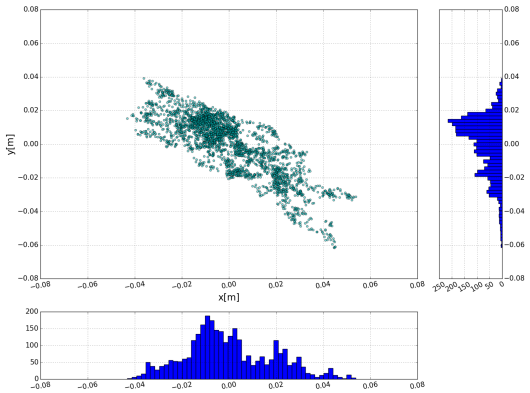


Fig. 6. Distribution of positioning data by QZSS

Based on these results, RTK-GPS can perform positioning more stably than QZSS in the stand-still state. One reason for this is the difference in the mechanism of position information correction, i.e., the base station is placed close

to the rover station in RTK-GPS. However, the errors of QZSS are less than approximately ± 4 cm and satisfy most applications of autonomous service robots. A more detailed discussion will be presented in Section III-D.

B. Measurement accuracy in motion in an open-sky environment

In-motion experiments were conducted by RTK-GPS and QZSS equipped in mobile robots. We compare the values measured by RTK-GPS and QZSS and the true values measured by a robotic total station (GPT-9005A, TOPCON Inc.). The measurement accuracy and frequency of the robotic total station are approximately ± 7 mm and 1.7 Hz, respectively. The latitude, longitude, and orientation of the robotic total station were measured using prism poles and QZSS (Fig. 8).

Fig. 7 shows the experimental environment, which is a square space of $18 \text{ m} \times 18 \text{ m}$, and the orange, green, and blue circles in Fig. 7 indicate the initial position of the mobile robot, the position of the robotic total station, and the position of the prism pole, respectively. In this experiment, the maximum linear velocity of the robot was set to 0.1 m/s for stable measurement using the total station.

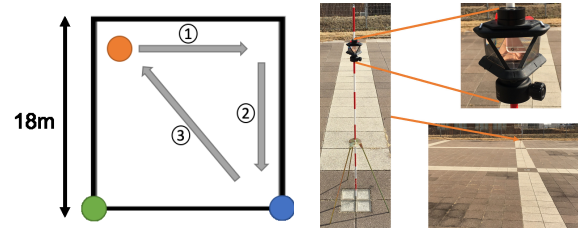


Fig. 7. Experimental conditions

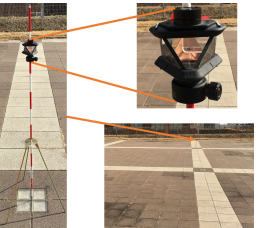


Fig. 8. Prism pole

The trajectories measured by the RTK-GPS, QZSS, and the robotic total station are shown in Figs. 9 and 10. In these figures, the green lines indicate the trajectories measured by the robotic total station, and blue lines indicate the trajectory measured by RTK-GPS or QZSS.

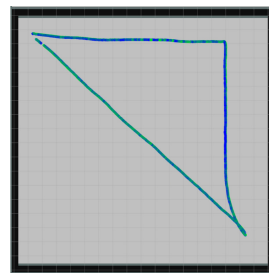


Fig. 9. Measured trajectories (green lines indicate the trajectories by the robotic total station, and blue lines indicate the trajectories by RTK-GPS)

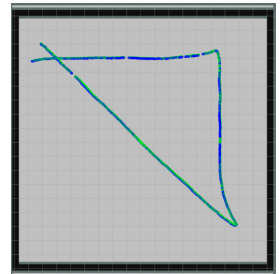


Fig. 10. Measured trajectories (green lines indicate the trajectories by the robotic total station, and blue lines indicate the trajectories by QZSS)

The maximum value (MAX), the root mean square (RMS), and the standard division (SD) of the differences between the positions measured by GNSS and the robotic total station are shown in Table I.

TABLE I
DIFFERENCES BETWEEN THE POSITIONS MEASURED BY GNSS AND THE
ROBOTIC TOTAL STATION

	RTK-GPS	QZSS
MAX [m]	0.085	0.115
RMS [m]	0.032	0.043
SD [m]	0.014	0.018

Based on this results, the accuracy of RTK-GPS is slightly higher than that of QZSS. A more detailed discussion is presented in Section III-D.

C. Experiment in a partially obscured environment

In this experiment, we run the robot along a route that is close to higher-rise buildings and compare the positioning accuracy and stability of RTK-GPS and QZSS. The results are shown in Figs. 11 and 12, respectively. Blue and green markers indicate Fixed and Float solutions, and orange markers indicate unstable solutions.

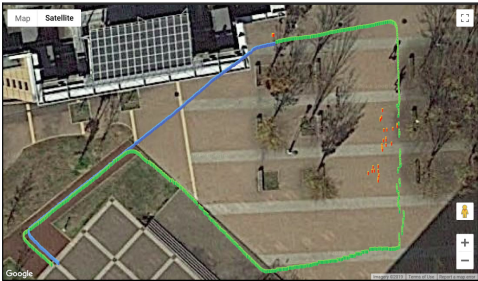


Fig. 11. Measured trajectory by RTK-GPS (blue and green markers indicate Fixed and Float solutions, and orange markers indicate unstable solutions)

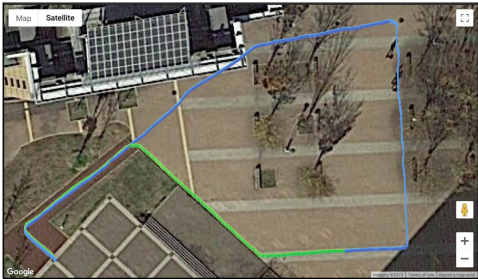


Fig. 12. Measured trajectory by QZSS (blue and green markers indicate Fixed and Float solutions, and orange markers indicate unstable solutions)

Based on these results, QZSS maintains a Fixed solution along most of the route and performs stable measurements, even when the robot passes near high-rise buildings. On the other hand, RTK-GPS becomes unstable in some cases. One reason for this is that QZSS uses the QZS placed at the quasi-zenith orbit and observed with a high elevation angle from the GNSS antenna. We repeated the experiment 10 times in the environment. Table II shows the Fixed rate, Float rate and Unstable rate for RTK-GPS and QZSS.

TABLE II

FIXED, FLOAT, AND UNSTABLE RATES FOR RTK-GPS AND QZSS

	RTK-GPS	QZSS
Fixed [%]	34.0	92.2
Float [%]	50.4	7.3
Unstable [%]	15.6	0.5

D. Performance comparison of RTK-GPS and QZSS

The performances of RTK-GPS and QZSS are shown in Table III. As a result of the experiments, we can see that RTK-GPS is more accurate than QZSS. The reason for this is thought to be the difference of the mechanism of position information correction. Correction information in RTK-GPS is created using the observation data at the base and the rover stations on-line. On the other hand, as mentioned above, QZSS utilizes the PPP-RTK (Precise Point Positioning RTK) method, which is one of the model-based techniques called SSR (State Space Representation). In PPP-RTK, the error is decomposed into the error in satellite clocks, a small variation in the orbit, tropospheric delay, ionospheric delay, etc., and these factors are estimated at the electronic reference points in CLAS of QZSS. However, PPP-RTK cannot take into account the real-time state change of errors and therefore can not handle, for example, the sudden change in ionospheric conditions.

As demonstrated by the results of the experiment in Section III, the positioning accuracy does not differ greatly between RTK-GPS and QZSS, and both techniques satisfy most of applications of autonomous service robots. Although RTK-GPS is slightly more accurate than RTK-GPS, QZSS requires two modules, and accurate positioning requires acquisition of the correct position of the base station. If the latitude and longitude of the base station are not accurately known, it takes a long time to obtain the accurate latitude and longitude by GNSS. We have to place the base station for a certain period of time and collect data repeatedly. In addition, since communication between the base station and the rover station is required, it can only be used within the range in which such communication is possible. On the other hand, since QZSS can perform a centimeter-class positioning with a single device, we do not need to consider an initialization procedure or the available range. Moreover, QZSS can perform more stable positioning, even near buildings because it uses satellites placed in a quasi-zenith orbit that are observed with a high elevation angle from the GNSS antenna. At any time, at least one QZS can always be observed in and around Japan. Consequently, we can conclude that QZSS is more suitable for a centimeter-class positioning system for autonomous service robots.

TABLE III
STATISTICS OF RTK-GPS AND QZSS

	RTK-GPS	QZSS
Accuracy (stopping)	◎ (Fixed)	○
Accuracy (moving)	◎ (Fixed)	○
Stability	△	◎
Number of modules	2	1
Initialization	Measurement of base position	None
Measurement range	In communication range between modules	Not limited (Around Japan)

With respect to the overall accuracy, RTK-GPS has a higher performance, but the difference is approximately several centimeters, which is not a large difference when considering the position identification of the robot. On the other hand, QZSS is superior with respect to the stability of

measurement, the number of required modules and preparations, the limits of the measurement range, and convenience. Overall, we conclude that QZSS is better for robot position identification.

IV. QUASI-ZENITH SATELLITE SYSTEM-BASED TOUR GUIDE ROBOT

As mentioned above, we confirmed that QZSS can perform centimeter-level positioning with a simple and easy-to-use system consisting of a single module. In this section, we introduce a tour guide robot as an example of an autonomous service robots using QZSS. Fig. 13 shows the developed tour guide robot.



Fig. 13. Photograph of the tour guide robot

A. System configuration

1) *Hardware configuration*: As a mobile platform, we used Loomo (Segway Inc.), which is an inverted two-wheeled robot, controlled from an Android terminal. We equipped Loomo with LDS-01 (ROBOTIS Inc.) and QZSS external sensors. LDS-01 is a low-cost 360-degree 2D-LiDAR used to detect obstacles. In addition, a battery, an external PC (Intel NUC), a Wi-Fi router for communication between Loomo and a PC are mounted on Loomo.

2) *Software configuration*: As software, a navigation system and the tour guide application are installed. The navigation system is based on the ROS Navigation Stack. Each component of the navigation system, localization, collision avoidance, and path planning is explained below.

- Localization: Position information obtained by QZSS and the velocity information measured by the wheel encoder are integrated by the extended Kalman filter (EKF) in robot_localization package [16]. EKF estimates the pose (position and yaw angle) and the velocity (linear and angular) of the robot.
- Collision avoidance: Using the data measured by LDS-01, the robot stops when a pedestrian is detected within a certain range.
- Path planning: The shortest path (global path) to the destination is planned using the Dijkstra method, and an optimal route (local path) to avoid obstacles is generated by the dynamic window approach along the global path.

In addition, as shown in Fig. 14, the tour guide application is implemented on the Android terminal. This application sends the goal information to the navigation system in

response to a request from the user and receives the current status of the robot. The status includes information such as whether the robot has reached the goal or an obstacle has been detected, and guide information for the attraction is provided by voice according to the location of the robot.

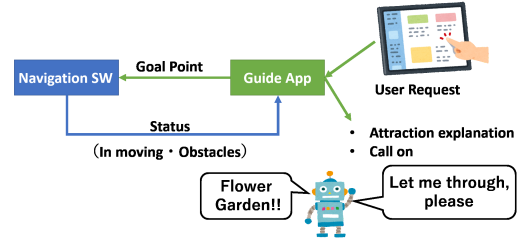


Fig. 14. Tour guide application

B. Tour guide experiment

We conducted a guided tour experiment to confirm the performance of the developed system at the "Huis Ten Bosch" theme park in Japan. The environment and the procedure of the experiment are shown in Fig. 15.

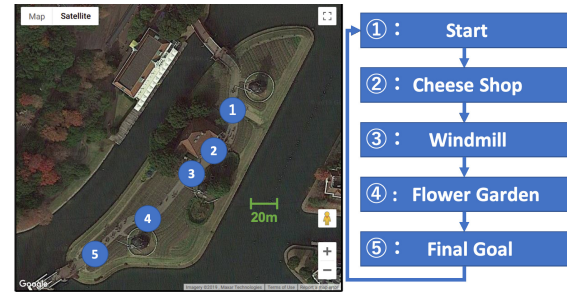


Fig. 15. Experimental environment and flow of guidance

The robot moves from point ① to point ⑤ and explains the attraction at each point by voice. The total distance traveled by the robot is approximately 130 meters, and the robot returns to the initial point, point ①, after arriving at point ⑤ automatically, as shown in Fig. 16.

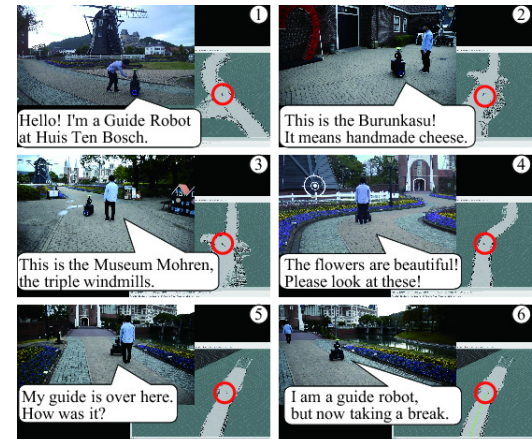


Fig. 16. Tour guide experiment

Fig. 16① shows the robot start the tour at the start position. In Fig. 16②, the robot arrives at the cheese shop, which

is the first target point, and gives a provide a description of it. Fig. 16③ shows the robot arriving at the windmill, which is the second target position, and providing an description of the windmill and the history of the Netherlands. In Fig. 16④, the robot arrives at the third target point, the flower garden, and provides a description of the types of flowers. In Fig. 16⑤, the robot arrives at the end point and announces the end of the tour. Fig. 16⑥ shows the robot returning to the start position after the tour is over.

Guided tour experiments were conducted seven times in total, and six of the tours were successfully performed as planned. The reason for the failure is that the measurement of QZSS became unstable in the area where buildings and trees were closely placed around the robot. However, this does not occur often, and, thus, if we plan the tour route carefully, the developed system is quite practical as a tour guide system for an outdoor theme park.

C. Experiment with the extended system

We conducted the tour guide demonstration as shown in Fig. 17. This system consists of the proposed tour guide robot system, 5G mobile communications system, and the AI-based voice interaction system. The robot status and the voice commands are transferred through the 5G network to the remote monitoring system and the cloud-based AI system in real-time. As shown in Fig. 17, the robot properly guided the guests to several sights requested by voice command.



Fig. 17. Experiment with the extended system

V. CONCLUSION

In the present paper, the performance of QZSS was examined, and its accuracy and stability was verified as a centimeter-level positioning system for autonomous service robots. In addition, we developed a practical tour guide robot system that can be used at an outdoor theme park. Experiments conducted at the theme park show that the tour guide robot successfully traveled 130 meters repeatedly and acted as a guide to the attractions using QZSS. The centimeter-level positioning service was started very recently from November 2018, and, to the best of our knowledge, this research is the first to use CLAS of QZSS for autonomous service robots. In the future, we intend to improve the stability of the developed tour guide robot system by combining sensors including not only on-board sensors, such as LRF

and cameras, but also ambient sensors embedded based on the concept of the informationally structured environment [17]. In addition, pedestrian detection and tracking are also important functions for a safe and efficient autonomous robot system, and we intend to implement these functions and develop a practical tour guide robot system in the future.

ACKNOWLEDGMENT

The present paper is based on results obtained from the "Cross-ministerial Strategic Innovation Promotion Program" (SIP), which was commissioned by the New Energy and Industrial Technology Development Organization (NEDO).

REFERENCES

- [1] G. Wan, X. Yang, R. Cai, H. Li, Y. Zhou, H. Wang, and S. Song, "Robust and precise vehicle localization based on multi-sensor fusion in diverse city scenes," in *2018 IEEE International Conference on Robotics and Automation (ICRA)*, pp. 4670–4677, May 2018.
- [2] M. Imperoli, C. Potena, D. Nardi, G. Grisetti, and A. Pretto, "An effective multi-cue positioning system for agricultural robotics," *IEEE Robotics and Automation Letters*, vol. 3, pp. 3685–3692, Oct 2018.
- [3] G. Patrick, E. Kevin, and H. Guoquan, "Asynchronous Multi-Sensor Fusion for 3D Mapping and Localization," in *2018 IEEE International Conference on Robotics and Automation (ICRA)*, 05 2018.
- [4] G. Kourous, I. Kotavelis, E. Skartados, D. Giakoumis, D. Tzovaras, A. Simi, and G. Manacorda, "3D Underground Mapping with a Mobile Robot and a GPR Antenna," in *2018 IEEE/RSJ International Conference on Intelligent Robots and Systems (IROS)*, pp. 3218–3224, Oct 2018.
- [5] J. Almeida, A. Ferreira, B. Matias, C. Lomba, A. Martins, and E. Silva, "iVAMOS! Underwater Mining Machine Navigation System," in *2018 IEEE/RSJ International Conference on Intelligent Robots and Systems (IROS)*, pp. 1520–1526, Oct 2018.
- [6] M.-A. Raúl and T. J. D., "ORB-SLAM2: an Open-Source SLAM System for Monocular, Stereo and RGB-D Cameras," *IEEE Transactions on Robotics*, vol. 33, no. 5, pp. 1255–1262, 2017.
- [7] J. Zhang and S. Singh, "LOAM: Lidar Odometry and Mapping in Real-time," in *Robotics: Science and Systems Conference*, July 2014.
- [8] T. Takasu and A. Yasuda, "Development of the low-cost RTK-GPS receiver with an open source program package RTKLIB," Jan 2009.
- [9] M. Saito, A. Yamagishi, J. Takiguchi, and K. Asari, "Introduction to High-Accuracy Satellite-based Positioning System utilizing QZSS," Tech. Rep. 26, Mitsubishi Space Software Co.,Ltd., 2016.
- [10] G. Bresson, Z. Alsayed, L. Yu, and S. Glaser, "Simultaneous localization and mapping: A survey of current trends in autonomous driving," *IEEE Transactions on Intelligent Vehicles*, vol. 2, pp. 194–220, Sep. 2017.
- [11] J. K. Suhr, J. Jang, D. Min, and H. G. Jung, "Sensor fusion-based low-cost vehicle localization system for complex urban environments," *IEEE Transactions on Intelligent Transportation Systems*, vol. 18, pp. 1078–1086, May 2017.
- [12] S. Fujita, M. Miya, and J. Takiguchi, "Establishment of Centimeter-class Augmentation System utilizing Quasi-Zenith Satellite System (Special Issue: Recent Topics on GNSS and Its Applications)," *System/Control/Information*, vol. 59, no. 4, pp. 126–131, 2015.
- [13] Cabinet Office (Japan), "Quasi-Zenith Satellite System Interface Specification Centimeter Level Augmentation Service Cabinet Office," tech. rep., 2018.
- [14] "Quasi-Zenith Satellite Orbit (QZO) | Technical Information | QZSS (Quasi-Zenith Satellite System) - Cabinet Office (Japan)," <http://qzss.go.jp/en/technical/technology/orbit.html>, February 2019.
- [15] G. Wübbena, M. Schmitz, and A. Bagge, "PPP-RTK : Precise Point Positioning Using State-Space Representation in RTK Networks," 2005.
- [16] M. Thomas and S. Daniel, "A Generalized Extended Kalman Filter Implementation for the Robot Operating System," in *roceedings of the 13th International Conference on Intelligent Autonomous Systems (IAS-13)*, Springer, July 2014.
- [17] J. Sakamoto, K. Kiyoyama, K. Matsumoto, Y. Pyo, A. Kawamura, and R. Kurazume, "Development of ros-tms 5.0 for informationally structured environment," *ROBOMECH Journal*, vol. 5, no. 24, 2018.